Dynamical phase transition of light in time-varying nonlinear dispersive media

Nicolas Cherroret*

Laboratoire Kastler Brossel, Sorbonne Université, CNRS, ENS-PSL Research University, Collège de France, 4 Place Jussieu, 75005 Paris, France

(Received 27 June 2023; accepted 5 January 2024; published 24 January 2024)

We demonstrate the existence of a prethermal dynamical phase transition (DPT) for fluctuating optical beams propagating in nonlinear dispersive media. The DPT can be probed by suddenly changing in time the dispersion and nonlinearity parameters of the medium (thus realizing a temporal interface), a procedure that emulates a quench in a massive φ^4 model. Above a critical value of the quench identifying the transition, the fluctuating beam after the temporal interface is characterized by a correlation length that diverges algebraically at the transition. Below the critical quench, the beam exhibits an algebraic relaxation and a self-similar scaling. Our analysis also reveals a dimensional crossover of the critical exponent, a characteristic feature of the optical DPT.

DOI: 10.1103/PhysRevA.109.013519

I. INTRODUCTION

In the nonequilibrium physics of isolated many-body systems, dynamical phase transitions (DPTs) have recently sparked considerable interest as examples of critical phenomena characterized by scaling properties different from their equilibrium counterparts. Loosely speaking, a DPT is associated with the emergence of distinct temporal evolutions of certain observables following a quantum quench. From this general definition, however, several qualitatively different types of DPTs have been identified. One type, for instance, arises in the time evolution of Loschmidt echoes, which may exhibit a cusp at a critical time upon quenching a parameter of the Hamiltonian, with the rate function of the echo vanishing at the critical time [1–3]. A second category of nonequilibrium critical phenomena has been observed for strong cooling quenches of three-dimensional quantum gases. Following the quench, the momentum distribution of the gas exhibits a universal, spatiotemporal self-similar scaling governed by a set of dynamical exponents [4–8]. A characteristic feature of this phenomenon, dubbed a nonthermal fixed point, is to be governed by the collisions between the quasiparticle excitations of the cold gas [9]. A third type of DPT finally, which is the subject of the present paper, arises in the so-called prethermal regime of many-body systems, where the quasiparticle collisions are, in contrast, mostly ineffective [10]. Prethermalization refers to an intermediate regime of times following a quench, where the dynamics is governed by excitations whose properties are renormalized by interactions but which can be considered independent. A prethermal dynamics naturally shows up, in particular, in weakly interacting systems close to integrability [11–16], as recently observed experimentally in cold-atom [17–19] and photonic [20] setups. In that context, a prethermal DPT corresponds to the emergence of qualitatively different dynamics of the system's correlations when quenching a control parameter of the Hamiltonian around a critical value [10]. Theoretically, prethermal DPTs have been described in particular in fully connected spin models [21–24] and in φ^4 field theories with $O(N)$ symmetry in the large-N limit [25–32]. On the experimental side, observations and characterizations of prethermal DPTs have been achieved with cold atoms, including trapped ions [33], atoms in optical cavities [34], Fermi gases [35], and spinor condensates [36,37].

In this paper we demonstrate theoretically the existence of a prethermal dynamical phase transition in a closed optical system made of a fluctuating light beam propagating in a nonlinear, dispersive dielectric medium. In recent decades, such optical platforms have been extensively investigated due to their ability to emulate with light the low-energy physics of quantum gases [38]. In particular, laser beams propagating in nonlinear atomic vapors [39] have proven to constitute a flexible tool to explore nonequilibrium phenomena such as thermalization [40,41], prethermalization and light-cone spreading [20], Zakharov-type oscillations [42], vortex dynamics [43], parametric resonances [44], and turbulence [45]. Likewise, in optical fibers the interplay between dispersion and nonlinearity has revealed interesting prethermal effects such as the Fermi-Pasta-Ulam-Tsingou recurrences [46,47] and an associated mechanism of broken symmetry [48].

The existence of an optical DPT discussed in the present work relies on the close resemblance between the wave equation governing light propagation in nonlinear dispersive media and the equation of motion of a massive classical φ^4 field theory. From this observation, we propose an optical quench protocol allowing us to trigger such a transition, based on a temporal change of the dispersion parameters of the medium (Sec. II), and we identify the precise condition under which the transition effectively occurs (Sec. III). In Sec. IV we then characterize the postquench dynamics of the optical beam above the transition point. This analysis, in particular, reveals the existence of two critical exponents characterizing the transition. In the close vicinity of the critical point, first, the critical exponent ν coincides with that of the equilibrium

*nicolas.cherroret@lkb.upmc.fr

quantum phase transition of the underlying two-dimensional φ^4 theory. When moving away from the transition, however, we find that ν crosses over to the value expected for an equilibrium quantum phase transition in dimension 3. This dimensional crossover is a characteristic feature of the optical DPT. Below the transition point, the dynamics exhibits scale invariance and self-similar scaling, which we describe both theoretically and analytically in Sec. V, following previous ideas developed in the context of the $O(N)$ model [25–32]. In Sec. VI we particularize the problem to a concrete system, a light beam propagating in a resonant atomic vapor, and deduce a possible phase diagram of the DPT in that type of medium. We summarize the paper in Sec. VII.

II. MODEL

A. Wave equation in nonlinear dispersive media

We consider an optical beam propagating in a dielectric medium in which the electric field is governed by the Helmholtz equation

$$\boldsymbol{\nabla} \times [\boldsymbol{\nabla} \times \mathbf{E}(\boldsymbol{r}, \omega)] = \frac{\omega^2}{c^2} \epsilon(\omega, \boldsymbol{r}) \mathbf{E}(\boldsymbol{r}, \omega), \tag{1}$$

where the relative permittivity $\epsilon(\omega, \boldsymbol{r}) = \epsilon_{\mathrm{L}}(\omega) + \epsilon_{\mathrm{NL}}(\boldsymbol{r})$ decomposes into a linear dispersive part $\epsilon_{\mathrm{L}}(\omega)$ and a nonlinear part $\epsilon_{\mathrm{NL}}(\boldsymbol{r}) \propto |\mathbf{E}|^2$ that depends quadratically on the wave field (Kerr effect). We further suppose that the beam is mostly directed along the axis z and that its spectrum is centered around a carrier frequency ω_0. This invites us to express the electric field as

$$\mathbf{E}(\boldsymbol{r}, t) = \mathrm{Re}[\boldsymbol{\mathcal{E}}(\boldsymbol{r}_\perp, z, t) e^{i(k_0 z - \omega_0 t)}], \tag{2}$$

where we isolated the envelope $\boldsymbol{\mathcal{E}}(\boldsymbol{r}_\perp, z, t)$, assumed to be a slowly varying function of the transverse $\boldsymbol{r}_\perp \equiv (x, y)$, longitudinal z, and temporal t coordinates. From now on, we assume that this envelope has a fixed polarization in the (x, y) plane and we focus on the evolution of the corresponding amplitude, denoted by $\mathcal{E}$. In Eq. (2) we also introduced the optical wave number $k_0 \equiv \sqrt{\epsilon_{\mathrm{L}}(\omega_0)}\omega_0/c$ at the carrier frequency, with c the speed of light in vacuum.

To account for the dispersion of the medium, we Taylor expand the linear part of the squared wave vector on the right-hand side (rhs) of Eq. (1) around ω_0 (slowly varying envelope approximation) [49],

$$k^2(\omega) \equiv \frac{\omega^2}{c^2} \epsilon_{\mathrm{L}}(\omega) \simeq k_0^2 + \frac{2k_0}{v}(\omega - \omega_0) + D(\omega - \omega_0)^2, \tag{3}$$

where $v \equiv (\partial k/\partial \omega)^{-1}$ is the group velocity and $D \equiv \frac{1}{2}(\partial^2 k^2/\partial \omega^2)$ is the quadratic dispersion parameter, which we assume to be positive from now on. Inserting Eqs. (2) and (3) into Eq. (1) and dropping terms involving second-order derivatives with respect to z (paraxial approximation), we find

$$\left(D\partial_t^2 - \Delta_\perp - 2ik_0\partial_z - \frac{2ik_0}{v}\partial_t - \frac{\omega_0^2}{c^2}\epsilon_{\mathrm{NL}}\right)\mathcal{E} = 0, \tag{4}$$

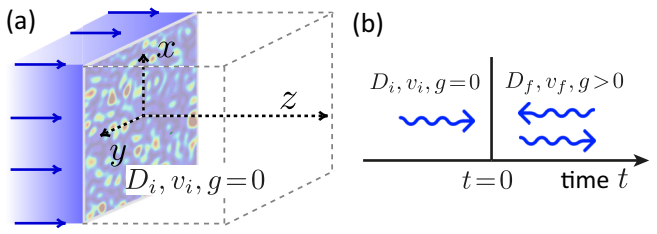

FIG. 1. (a) Optical beam propagating for $t < 0$ in a dispersive dielectric medium with dispersion parameters D_i and v_i and no nonlinearity. The wave is assumed to exhibit spatial fluctuations in the (x, y) plane, as well as frequency fluctuations (not shown in the figure). (b) At $t = 0$, we suppose that the dispersion and nonlinearity parameters are suddenly quenched from $(D_i, v_i, g = 0)$ to $(D_f, v_f, g > 0)$. This defines a temporal interface, beyond which two waves propagating forward and backward in time emerge.

where $\Delta_\perp$ is the Laplace operator in the transverse plane (x, y). As a last step, we introduce the new field variable

$$\phi(\boldsymbol{r}_\perp, z, t) \equiv \mathcal{E}(\boldsymbol{r}_\perp, z, t) e^{-i\mu t}, \tag{5}$$

where $\mu \equiv k_0/Dv$. In this frame, the wave equation becomes

$$\left(D\partial_t^2 - \Delta_\perp - 2ik\partial_z + \frac{k_0^2}{Dv^2} + g|\phi|^2\right)\phi(\boldsymbol{r}_\perp, z, t) = 0, \tag{6}$$

where we defined the nonlinear parameter g such that $-(\omega_0^2/c^2)\epsilon_{\mathrm{NL}} \equiv g|\phi|^2$. In the following, we suppose $g > 0$, corresponding to a defocusing nonlinearity.

At this stage, it is interesting to note that the wave equation (6) resembles a nonlinear Klein-Gordon-type equation, i.e., the equation of motion of a classical massive φ^4 theory with coupling constant g and mass k_0^2/Dv^2. Generally speaking, the φ^4 field theory is a prototypical model describing the large-scale behavior of a broad range of systems near a second-order equilibrium phase transition separating a disordered and an ordered phase [50,51]. In the present context though, the propagating wave is *a priori* not in a state of thermal equilibrium, so probing such a phase transition with light is not obvious. The φ^4 model, nevertheless, is also known to host a dynamical phase transition [10,25,26], which does not necessarily require one to start from a thermal state. Such a DPT usually arises when performing a temporal change (quench) of a control parameter (often the mass) around a certain critical value. Following the quench, the system exhibits distinctive dynamical evolutions on each side of this critical point. In the following sections we give consistency to this discussion by introducing a physical protocol allowing us to probe a DPT of that type with light governed by the wave equation (6).

B. Prequench optical state and quench protocol

To probe the optical DPT behind Eq. (6), we consider a fluctuating beam initially propagating for $t < 0$ in a dispersive medium with $v = v_i$, $D = D_i > 0$, and no nonlinearity $(g = 0)$ [see Fig. 1(a)]. Defining the Fourier transform

$\phi(\boldsymbol{q}_\perp, z, \omega) \equiv \int d^2\boldsymbol{r}_\perp \int dt\, \phi(\boldsymbol{r}_\perp, z, t) e^{-i\boldsymbol{q}_\perp\cdot\boldsymbol{r}_\perp + i\omega t}$, we assume that the spectrum of the beam at $z = 0$ takes the form

$$\phi^{(0)}(\boldsymbol{q}_\perp, \omega) \equiv \phi(\boldsymbol{q}_\perp, z = 0, \omega) = \sqrt{I}\phi_T(\boldsymbol{q}_\perp)\phi_F(\omega), \tag{7}$$

where I is the beam intensity and ϕ_T and ϕ_F are random fields with independent statistics, which encode spatial fluctuations in the transverse plane and frequency fluctuations, respectively. In practice, the spatial fluctuations can be obtained by, e.g., imprinting a speckle pattern onto the wavefront of a laser [20], while the frequency fluctuations are associated with deviations of the beam from pure monochromaticity. As the first property of these fluctuations, we impose that the statistical average of the field $\phi^{(0)}$ vanishes, which is realized, for instance, by setting

$$\langle \phi_T(\boldsymbol{q}_\perp)\rangle = 0. \tag{8}$$

Defined in this way, the optical field for $t < 0$ can be seen as a kind of optical analog to a thermal system belonging to a disordered phase. We further suppose that the spatial and frequency fluctuations are translationally invariant and stationary, respectively, i.e., their two-point correlators obey

$$\langle \phi_T^*(\boldsymbol{q}_\perp)\phi_T(\boldsymbol{q}'_\perp)\rangle = \delta^2(\boldsymbol{q}_\perp - \boldsymbol{q}'_\perp) S_T(\boldsymbol{q}_\perp) \tag{9}$$

and

$$\langle \phi_T^*(\omega)\phi_T(\omega')\rangle = \delta(\omega - \omega') S_F(\omega). \tag{10}$$

These relations also define the spatial and frequency fluctuation spectra $S_T(\boldsymbol{q}_\perp)$ and $S_F(\omega)$, which we choose normalized: $\int d^2\boldsymbol{q}_\perp/(2\pi)^2 S_T(\boldsymbol{q}_\perp) = \int d\omega/2\pi S_F(\omega) = 1$. In the quench protocol presented below, we will see that the spatial spectrum can be traced out of the description such that there is no need to specify its exact shape at this stage. As for the frequency spectrum, in the following we consider the simple Lorentzian shape

$$S_F(\omega) = \frac{2\gamma}{(\omega - \mu)^2 + \gamma^2} \tag{11}$$

of bandwidth γ. Notice that $S_F(\omega)$ is centered around $\omega = \mu$, which corresponds to a spectrum of the original field $\mathbf{E}$ centered around the carrier frequency ω_0 by virtue of the definitions (2) and (5).

To trigger a DPT in that system, the key idea is to perform a temporal change of the optical parameters that emulates a quench from the disordered to the ordered phase in the underlying φ^4 theory [10]. To achieve this goal, we assume that, at $t = 0$, the dispersion parameters (v, D) and the nonlinear strength g of the medium are suddenly changed according to the protocol

$$(D_i > 0, v_i, g = 0) \to (D_f > 0, v_f, g > 0), \tag{12}$$

where D_f and v_f can, at this stage, *a priori* take arbitrary positive values.[1] Note that, from the physical point of view, this quench protocol defines a time-varying interface in the dielectric medium at $t = 0$, as illustrated in Fig. 1(b). This interface generically gives rise, for $t > 0$, to two waves propagating forward and backward in time, analogously to the well-known transmitted and reflected waves arising at a spatial interface between two dielectric media [52]. We will discuss this interpretation more quantitatively at the end of Sec. IV A.

The wave field in the prequench regime $t < 0$, which is solution of the wave equation (6), explicitly reads

$$\phi(\boldsymbol{r}_\perp, z, t < 0) = \iint \frac{d\omega}{2\pi}\frac{d^2\boldsymbol{q}_\perp}{(2\pi)^2}\phi(\boldsymbol{q}_\perp, 0, \omega) e^{i\boldsymbol{q}_\perp\cdot\boldsymbol{r}_\perp - i\omega t} \times \exp\left[-\frac{iz}{2k}\left(\boldsymbol{q}_\perp^2 - D_i\omega^2 + \frac{k_0^2}{D_i v_i^2}\right)\right]. \tag{13}$$

Note that, due to the assumed factorized spectrum (7) of the initial fluctuations, this solution is of the form $\phi(\boldsymbol{r}_\perp, z, t < 0) = \varphi_T(\boldsymbol{r}_\perp, z)\varphi(z, t)$, i.e., the transverse fluctuations decouple from the dynamics. A similar situation is encountered in optical fibers, which could also be a good candidate to implement the present scheme. In that case, ϕ_T would correspond to a transverse mode of the fiber, and the condition of a vanishing mean field (8) would be achieved by averaging over the azimuthal phase of that mode. Starting from this optical state and from the quench protocol (12), in the next section we examine the dynamical evolution of the wave field for $t > 0$.

III. DYNAMICAL PHASE TRANSITION OF LIGHT

A. Mean-field postquench dynamics

To find the solution of the wave equation (6) for $t > 0$, we use the ansatz

$$\phi(\boldsymbol{r}_\perp, z, t > 0) = \iint \frac{d\omega}{2\pi}\frac{d^2\boldsymbol{q}_\perp}{(2\pi)^2}\phi^{(0)}(\boldsymbol{q}_\perp, \omega) e^{i\boldsymbol{q}_\perp\cdot\boldsymbol{r}_\perp} f_\omega(t) \times \exp\left[-\frac{iz}{2k}\left(\boldsymbol{q}_\perp^2 - D_i\omega^2 + \frac{k_0^2}{D_i v_i^2}\right)\right], \tag{14}$$

which has essentially the same form as Eq. (13) except for the unknown function $f_\omega(t)$. The latter can be found by imposing that Eq. (14) is solution of the wave equation (6) with $D = D_f$, $v = v_f$, and $g \neq 0$. This yields

$$\iint \frac{d\omega}{2\pi}\frac{d^2\boldsymbol{q}_\perp}{(2\pi)^2}\phi^{(0)}(\boldsymbol{q}_\perp, \omega) \times \exp\left[i\boldsymbol{q}_\perp\cdot\boldsymbol{r}_\perp - \frac{iz}{2k_0}\left(\boldsymbol{q}_\perp^2 - D_i\omega^2 + \frac{k_0^2}{D_i v_i^2}\right)\right] \times \left[D_f\ddot{f}_\omega(t) + \left(D_i\omega^2 + \frac{k_0^2}{D_f v_f^2} - \frac{k_0^2}{D_i v_i^2}\right) f_\omega(t)\right] + g|\phi|^2\phi = 0. \tag{15}$$

[1] Strictly speaking, the variations of dispersion parameters cannot be infinitely fast, so the slowly varying envelope approximation underlying Eq. (4) remains valid. A condition for D, e.g., is that $|\partial_t D| \ll 2k_0/v$. In terms of the quench duration t_q, this gives the condition $\mu t_q \gg |m| = |1 - v_f/v_i|$. For example, for the numerical parameters chosen in Fig. 2, $|m| \sim 0.2$ so that the assumption of sudden quench is in fact restricted to $0.2 \ll \mu t_q \ll t$.

When evaluated with the ansatz (14), the last nonlinear term $g|\phi|^2\phi$ on the left-hand side involves products of three random fields $\phi^{(0)}$ at different momenta and frequencies. To simplify it, we employ a mean-field Hartree-Fock-Bogoliubov approximation, a truncation scheme that consists in neglecting all correlation functions beyond the second one [53]. While this scheme cannot capture the long-time evolution after the quench, it is known to accurately describe the intermediate timescales, i.e., the prethermal dynamics, where a DPT is expected to take place. In the term $g|\phi|^2\phi$, this approximation amounts to applying the factorization rule

$$\begin{aligned}&\phi^{(0)*}(\boldsymbol{q}_1,\omega_1)\phi^{(0)}(\boldsymbol{q}_2,\omega_2)\phi^{(0)}(\boldsymbol{q}_3,\omega_3)\\&\quad\to\langle\phi^{(0)*}(\boldsymbol{q}_1,\omega_1)\phi^{(0)}(\boldsymbol{q}_2,\omega_2)\rangle\phi^{(0)}(\boldsymbol{q}_3,\omega_3)\\&\qquad+\langle\phi^{(0)*}(\boldsymbol{q}_1,\omega_1)\phi^{(0)}(\boldsymbol{q}_3,\omega_3)\rangle\phi^{(0)}(\boldsymbol{q}_2,\omega_2).\end{aligned}\tag{16}$$

Making use of Eqs. (9) and (10) and invoking the normalization condition for $S_T(\boldsymbol{q}_\perp)$, we infer

$$\begin{aligned}g|\phi|^2\phi\simeq 2gI&\iint\frac{d\omega}{2\pi}\frac{d^2\boldsymbol{q}_\perp}{(2\pi)^2}\phi^{(0)}(\boldsymbol{q}_\perp,\omega)\\&\times\int\frac{d\omega'}{2\pi}S_F(\omega')|f_{\omega'}(t)|^2\\&\times\exp\left[i\boldsymbol{q}_\perp\cdot\boldsymbol{r}_\perp-\frac{iz}{2k_0}\left(\boldsymbol{q}_\perp^2-D_i\omega^2+\frac{k_0^2}{D_iv_i^2}\right)\right].\end{aligned}\tag{17}$$

Inserting this relation into Eq. (15), we finally obtain a closed equation for $f_\omega(t)$,

$$\ddot{f}_\omega(t)+\left(\frac{D_i}{D_f}\omega^2+m_{\rm eff}(t)\right)f_\omega(t)=0,\tag{18}$$

where

$$m_{\rm eff}(t)\equiv m+\frac{2gI}{D_f}\int_{-\infty}^{\infty}\frac{d\omega}{2\pi}S_F(\omega)|f_\omega(t)|^2,\tag{19}$$

with $m\equiv k_0^2/(D_fv_f)^2-k_0^2/D_iD_fv_i^2$. The nonlinear equation (18) must be complemented by initial conditions, which we find by ensuring the continuity of the field envelope $\mathcal{E}$ and of its time derivative at the temporal interface. From the prequench solution (13), these conditions yield

$$f_\omega(0)=1,\quad \dot{f}_\omega(0)=-i(\omega+\mu_i-\mu_f),\tag{20}$$

where the factor $\mu_i-\mu_f=k_0/D_iv_i-k_0/D_fv_f$ stems from the phase relating the variables ϕ and $\mathcal{E}$ [see Eq. (5)], which changes from μ_it to μ_ft when the quench is performed.

In statistical physics, equations of the form of (18) have been studied in the context of quenches in the $O(N)$ model, for which they constitute the exact solution in the limit $N\to\infty$ [25–31]. In that framework, m is the mass parameter of the free theory ($g=0$), which becomes self-consistently renormalized to $m_{\rm eff}(t)$ when g is nonzero. In the present optical problem, $m_{\rm eff}(t)$ is a crucial quantity for the dynamics, which in turn is related to the total wave intensity after the quench through

$$\langle|\phi(\boldsymbol{r}_\perp,z,t)|^2\rangle=\int\frac{d\omega}{2\pi}S_F(\omega)|f_\omega(t)|^2=\frac{m_{\rm eff}(t)-m}{2gI/D_f},\tag{21}$$

where the first equality follows from Eq. (14), using Eqs. (9) and (10). A core property of the equation of motion (18) is that if m is chosen to be negative (which is realized for $D_fv_f^2>D_iv_i^2$), the effective mass $m_{\rm eff}(t)$ may vanish at long time and induce a dynamical phase transition [25]. The precise condition for this to happen is discussed in the next section.

It is interesting to notice, finally, that the initial transverse fluctuations have been completely traced out in the derivation of Eq. (18). This means that their precise properties are of no importance for the postquench dynamics, which is solely governed by the frequency fluctuations. This decoupling originates from the factorization of spatial and frequency fluctuations that we assumed for the incoming wave [Eq. (7)], as discussed at the end of Sec. II B. In fact, the essential role of the transverse fluctuations is here to guarantee that the mean field vanishes $\langle\phi(t)\rangle=0$, due to Eq. (8), so as to mimic a prequench state lying in a disordered phase. In the case of a nonzero initial mean field, the equation of motion (19) would be modified and should be complemented by an additional equation governing the dynamics of $\langle\phi(t)\rangle$.

B. Dynamical phase transition

In [54] it was shown that in nonlinear equations of the type of Eq. (18), the effective mass $m_{\rm eff}(t)$ generically converges at long time to a constant positive value $m_{\rm eff}(\infty)$. A dynamical phase transition then exists if $m_{\rm eff}(\infty)$ vanishes for a certain critical (negative) value m_c of the quench parameter m. To find out whether such a DPT is present in the model of (18) and (19), we use an ansatz originally proposed in [27,54] for calculating $m_{\rm eff}(\infty)$: We replace the stationary value of $|f_\omega(t)|^2$ on the rhs of Eq. (19) by the result of the free theory ($g=0$) self-consistently evaluated at $m=m_{\rm eff}(\infty)$. Since the solution of the free theory is

$$\begin{aligned}f_\omega^{\rm free}(t)=&\cos(t\sqrt{\omega^2D_i/D_f+m})\\&-\frac{i(\omega+\mu_i-\mu_f)}{\sqrt{\omega^2D_i/D_f+m}}\sin(t\sqrt{\omega^2D_i/D_f+m}),\end{aligned}\tag{22}$$

this ansatz leads to

$$\begin{aligned}m_{\rm eff}(\infty)=m+\frac{2gI}{D_f}&\int\frac{d\omega}{2\pi}S_F(\omega)\\&\times\frac{(\omega+\mu_i-\mu_f)^2+\omega^2D_i/D_f+m_{\rm eff}(\infty)}{2[\omega^2D_i/D_f+m_{\rm eff}(\infty)]}.\end{aligned}\tag{23}$$

A DPT, if it exists, corresponds to a critical value $m=m_c$ for which $m_{\rm eff}(\infty)=0$. This imposes that

$$m_c=-\frac{gI}{D_i}\int\frac{d\omega}{2\pi}S_F(\omega)\frac{(\omega+\mu_i-\mu_f)^2+\omega^2D_i/D_f}{\omega^2}.\tag{24}$$

In this relation, the frequency integral on the rhs is nondivergent at $\omega\to0$ only when $\mu_i=\mu_f$. This is the phase-matching condition required for the dispersive medium to display a DPT after the quench, which we assume to be fulfilled from now on:

$$\mu_i=\mu_f\equiv\mu\Leftrightarrow D_iv_i=D_fv_f.\tag{25}$$

The phase-matching condition allows us to rewrite the equation of motion (18) in the dimensionless form

$$\ddot{f}_\omega(t) + \left(\frac{v_f}{v_i}\omega^2 + m_{\rm eff}(t)\right) f_\omega(t) = 0,$$
$$m_{\rm eff}(t) = m + \frac{\lambda}{2}\int_{-\infty}^{\infty}\frac{d\omega}{2\pi}\frac{2\gamma}{(\omega-1)^2+\gamma^2}|f_\omega(t)|^2, \tag{26}$$

where we introduced $\lambda \equiv 4gI/D_f\mu^2$. The mass parameter is now $m \equiv 1 - v_f/v_i$, and time and frequency are expressed in units of μ^{-1} and μ, respectively. Note that this equation of motion depends on three independent parameters only: the nonlinear coupling strength λ, the spectral width γ, and the ratio v_f/v_i of group velocities before and after the quench, this ratio being the natural control parameter allowing us to explore the DPT. Equation (26) is also the form that will be used in our numerical simulations below. At the phase-matching condition (25), the critical quench (24) at which the DPT occurs can be rewritten in terms of a critical value $v_f/v_i|_c$,

$$m_c \equiv 1 - \left.\frac{v_f}{v_i}\right|_c = -\frac{\lambda}{4}\frac{1+v_f/v_i|_c}{v_f/v_i|_c}, \tag{27}$$

which yields the critical ratio of group velocities

$$\left.\frac{v_f}{v_i}\right|_c = \frac{1}{8}[4+\lambda+\sqrt{16+\lambda(24+\lambda)}]. \tag{28}$$

In the next two sections, we characterize the general properties of the solutions of Eq. (26) in the vicinity of the critical quench, i.e., for $m > m_c$ and $m < m_c$, corresponding to $v_f/v_i < v_f/v_i|_c$ and $v_f/v_i > v_f/v_i|_c$, respectively. The practical realization of the critical ratio (28) for a concrete example of dispersive medium will be discussed in Sec. VI.

IV. QUENCH ABOVE THE CRITICAL POINT

A. Divergence of the correlation length

We first show in Fig. 2 the effective mass $m_{\rm eff}(t)$ as a function of time, obtained by solving Eq. (26) numerically for a few values of m above m_c. As announced, following the quench, the effective mass quickly saturates at a finite value $m_{\rm eff}(\infty)$ that gets closer and closer to zero as m approaches m_c. The saturation value is well described by the solution of Eq. (23), shown as dashed lines.

Above the DPT, the saturation value of the effective mass defines a correlation length $\xi \equiv 1/\sqrt{m_{\rm eff}(\infty)}$, which diverges algebraically near the critical point. Figure 3 shows ξ as a function of the distance $m - m_c$ to the critical point, for different values of the bandwidth γ of the frequency spectrum. Whatever γ is, we find that ξ diverges algebraically at $m = m_c$, which is a hallmark of the DPT. The numerical results of Fig. 3, however, also demonstrate the existence of a crossover between two algebraic scaling laws in the region $0 < m - m_c \ll 1$. Indeed, above a small but finite value of $m - m_c$ we find $\xi \sim 1/(m-m_c)^{1/2}$, whereas below that value we have $\xi \sim 1/(m-m_c)$, a scaling which persists up to arbitrarily small $m - m_c$. The existence of this crossover is a characteristic feature of the optical DPT. It is in turn due to the competition between two antagonistic effects: on the one hand, the approach to the DPT, whose critical properties

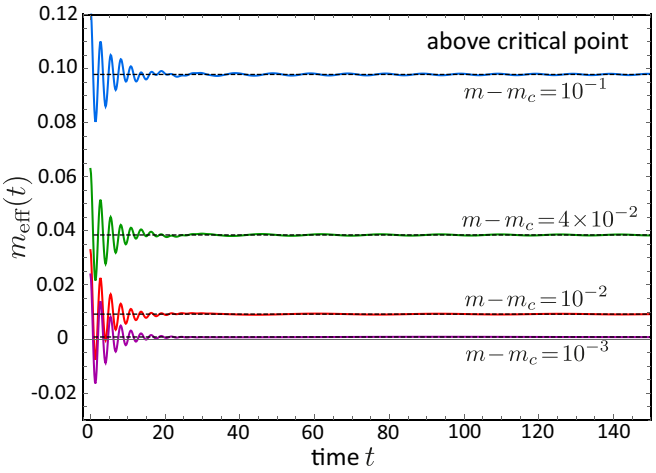

FIG. 2. Effective mass $m_{\rm eff}(t)$ vs time for a few values of the quench parameter m above its critical value m_c, for $\lambda = 0.5$ and $\gamma = 0.1$. At long time $m_{\rm eff}(t)$ converges to a finite positive value $m_{\rm eff}(\infty)$. The latter is well captured by the solution of Eq. (23), shown as black dashed lines. Here time and frequency are in units of μ^{-1} and μ, respectively, and m, m_c, and $m_{\rm eff}(t)$ are in units of μ^2.

are governed by the infrared frequency limit $\omega \to 0$, and, on the other hand, the frequency spectrum of the beam, which selects the finite frequency $\omega = 1$ [see Eq. (26)]. This can be explicitly demonstrated by combining Eqs. (23)–(25) to express $m_{\rm eff}(\infty)$ as a function of $m - m_c$:

$$m_{\rm eff}(\infty) = m - m_c - \frac{\lambda}{2}\int\frac{d\omega}{2\pi}\frac{S_F(\omega)m_{\rm eff}(\infty)}{2\frac{v_f}{v_i}[\frac{v_f}{v_i}\omega^2 + m_{\rm eff}(\infty)]}. \tag{29}$$

The existence of the crossover between to critical behaviors becomes clear if one notices that the value of the integral on the rhs depends on which of the functions $S_F(\omega)$ or

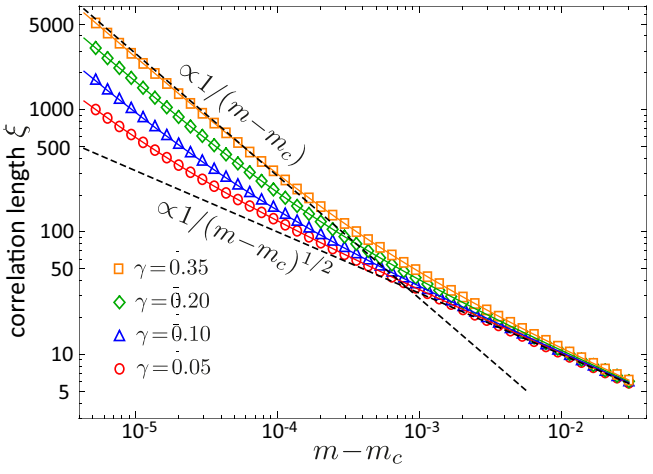

FIG. 3. Correlation length $\xi \equiv 1/\sqrt{m_{\rm eff}(\infty)}$ as a function of the distance $m - m_c$ to the critical point, for different values of the bandwidth γ. Symbols are numerical results, obtained by solving Eq. (26). The dashed lines show the asymptotic analytical predictions (30) and (31) in the close vicinity of the DPT and slightly away from it. Here $\lambda = 0.5$ and the parameter units are the same as in Fig. 2.

$[\frac{v_f}{v_i}\omega^2 + m_{\rm eff}(\infty)]^{-1}$ is the narrowest. At very small $m - m_c$, it is the second one, which selects the infrared frequencies and eventually yields, to leading order in $m_{\rm eff}(\infty) \ll 1$,

$$\xi \equiv \frac{1}{\sqrt{m_{\rm eff}(\infty)}} \simeq \frac{1}{m - m_c} \frac{\lambda S_F(0)}{8} \frac{v_i}{v_f}\bigg|_c^{3/2}. \tag{30}$$

On the other hand, at larger $m - m_c$ the frequency spectrum becomes more peaked, so the frequency region around $\omega = 1$ becomes the dominant contribution to the integral. As a result, the second term on the rhs of Eq. (29) becomes subleading and we find instead

$$\xi \simeq \frac{1}{\sqrt{m - m_c}}. \tag{31}$$

The two asymptotic laws (30) and (31) are displayed in Fig. 3 (dashed lines). They match very well the numerical results without any fit parameter. The crossover point separating the two regimes is readily obtained by equating the asymptotes. We find $m - m_c \simeq \lambda^2\gamma^2/16$.

Let us finally discuss the distribution function $f_\omega(t)$ above the critical point. Since the effective mass saturates at long time, $f_\omega(t)$ is approximately given by

$$f_\omega(t) \simeq \cos(t\sqrt{\omega^2 + \xi^{-2}}) - \frac{i\omega \sin(t\sqrt{\omega^2 + \xi^{-2}})}{\sqrt{\omega^2 + \xi^{-2}}}, \tag{32}$$

where we used that v_f/v_i is close to one in the vicinity of the critical point. Returning to the physical problem of light propagation, we see that this solution actually describes the superposition of two optical waves propagating forward and backward in time for $t > 0$. This phenomenon, illustrated in Fig. 1(b), is characteristic of waves scattered from time-varying dielectric interfaces (see, e.g., [52] for a review).

B. Link to the $O(N)$ model and dimensional crossover

The two asymptotic laws (30) and (31) can be recast as $\xi \sim (m - m_c)^{-\nu}$, with a critical exponent ν crossing over from 1 to $\frac{1}{2}$ when moving away from the transition. To better understand this crossover, it is instructive to make a connection with the critical properties of the usual quantum (i.e., zero-temperature) equilibrium phase transition of the φ^4 model with $O(N)$ symmetry that we recall here. The $O(N)$ model describes an N-component scalar field $\mathbf{\Phi}$ in dimension d with the Hamiltonian [27,28,51]

$$H = \int d^dx \frac{1}{2}\big(\mathbf{\Pi}^2 + (\nabla\mathbf{\Phi})^2 + m\mathbf{\Phi}^2 + \frac{u}{12N}(\mathbf{\Phi}^2)^2\big), \tag{33}$$

where $\mathbf{\Pi}$ is the canonical conjugate momentum of $\mathbf{\Phi}$ (for simplicity we use the same denotation m for the mass parameter as in the optical problem). In the limit $N \to \infty$, a Hartree approximation similar to that we used in Sec. III A allows us to exactly map the Hamiltonian (33) onto a quadratic one with effective mass self-consistently given by [27,51]

$$m_{\rm eff} = m + \frac{u}{12}\int \frac{d^d\boldsymbol{q}}{(2\pi)^d} \frac{1}{\sqrt{\boldsymbol{q}^2 + m}}, \tag{34}$$

where $|\boldsymbol{q}|$ is supposed to be bounded from above by an ultraviolet cutoff. This equation similarly defines an equilibrium quantum critical point $m_c = -(u/12)\int d^d\boldsymbol{q}/(2\pi)^d/|\boldsymbol{q}|$ where

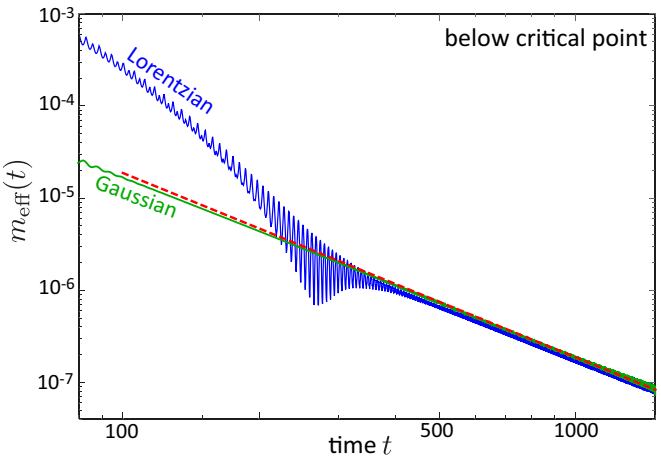

FIG. 4. Effective mass $m_{\rm eff}(t)$ vs time obtained by solving numerically Eq. (26) for $m - m_c = -0.3$ and $\lambda = 4$. The blue and green curves show numerical results for a Lorentzian spectrum (with $\gamma = 0.1$) and a Gaussian spectrum (with $\gamma = 0.45$), respectively. The red dashed line is the analytical prediction (41), a consequence of scale invariance below the critical point. Here time and frequency are in units of μ^{-1} and μ, respectively, and m, m_c, and $m_{\rm eff}(t)$ are in units of μ^2.

$m_{\rm eff} = 0$, showing that a transition only exists when $d > 1$. In that case, the correlation length $\xi \equiv \sqrt{m_{\rm eff}}^{-1}$ in the vicinity of the critical point obeys the algebraic law $\xi \sim (m - m_c)^{-\nu}$ with

$$\nu = \frac{1}{d-1} \quad (1 < d < 3), \qquad \nu = \frac{1}{2} \quad (d \geqslant 3). \tag{35}$$

A comparison with Eq. (30) suggests that the critical exponent of the optical DPT in dispersive media when $m - m_c \to 0$ is the same as the one of second-order equilibrium quantum phase transitions in dimension 2. Furthermore, the smooth change of the critical exponent from 1 to $\frac{1}{2}$ observed in Fig. 3 can be seen as a dimensional crossover, where the class of the optical DPT turns from that of a quantum phase transition in dimension 2 to that of a quantum phase transition in dimension 3 (the upper critical dimension) as one moves away from the critical point. In recent works [28,29], a somewhat related quantum-to-classical crossover (but at fixed spatial dimension) was reported, but a dimensional crossover in a DPT is a different phenomenon. As mentioned in the previous section, it stems from the peculiar shape of the fluctuation spectrum (11), which selects out a nonzero frequency when the spectral width γ is small enough. Previous works on DPTs in the $O(N)$ models, on the contrary, have so far been restricted to fluctuation spectra centered on $\omega = 0$ [29].

V. QUENCH BELOW THE CRITICAL POINT

A. Scale invariance

Let us now consider quenches below the critical point, namely, $m < m_c$ (or $v_f/v_i > v_f/v_i|_c$). Numerical resolution of Eq. (26) for $m_{\rm eff}(t)$ in that case is shown in Fig. 4. After a transient regime, one finds that the effective mass decays algebraically as $m_{\rm eff} \sim 1/t^2$. Such a behavior was previously reported in the context of the $O(N)$ model in the limit

$N \to \infty$, where it was found to be associated with scale invariance [29]. To show this, let us consider a rescaling $(t \to \epsilon t, \omega \to \omega/\epsilon)$ of the time and frequency variables in Eq. (26). The rescaled equation reads

$$\frac{1}{\epsilon^2}\ddot{f}_{\omega/\epsilon}(\epsilon t) + \left(\frac{v_f}{v_i}\frac{\omega^2}{\epsilon^2} + m_{\rm eff}(\epsilon t)\right) f_{\omega/\epsilon}(\epsilon t) = 0. \tag{36}$$

A comparison with Eq. (26) immediately shows that scale invariance is achieved when $m_{\rm eff}(\epsilon t) = (1/\epsilon^2) m_{\rm eff}(t)$, i.e., when $m_{\rm eff}(t) \propto 1/t^2$, in agreement with the numerical observation of Fig. 4. Scale invariance is thus a core dynamical property of nonlinear dispersive medium below the critical quench. Below we show how this feature manifests in the scaling properties of the distribution function $f_\omega(t)$.

B. Scaling properties of the distribution function

The scale-invariance property of the equation of motion below the critical point is expected to give rise to a specific universal self-similar behavior of the distribution function $f_\omega(t)$. To disclose this behavior, we look for asymptotic expressions of the solution of Eq. (26) in the regime of scale invariance where $m_{\rm eff}(t) = a/t^2$, with a a numerical constant to be determined. In the context of the $O(N)$ model, a methodology to achieve this goal was proposed in [29] in a particular deep-quench limit where the initial conditions for f_ω and $\dot{f}_\omega$ are constant. This is not the case in the present optical DPT, which requires us to adapt the method of [29], as we now discuss.

For $\omega \geqslant 0$, the general solution of Eq. (26) with $m_{\rm eff}(t) = a/t^2$ is given by

$$f_\omega(t) = \sqrt{\omega t}\left[A_\omega J_\alpha\left(\sqrt{\frac{v_f}{v_i}}\omega t\right) + B_\omega J_{-\alpha}\left(\sqrt{\frac{v_f}{v_i}}\omega t\right)\right], \tag{37}$$

where $\alpha = \sqrt{1/4 - a}$ and A_ω and B_ω are coefficients to be found. This solution is only expected to hold beyond a certain timescale t_0 beyond which scale invariance emerges.[2] Therefore, to find A_ω and B_ω we cannot directly use the initial conditions for f_ω, but instead we should to match the solution (37) with an approximate expression of $f_\omega(t)$ at $t = t_0$ [29]. To find the latter, we extrapolate from the initial condition using the Taylor expansion $f_\omega(t_0) = f_\omega(0) + t_0 \dot{f}_\omega(0) + O(t_0^2)$. From Eq. (20) we infer

$$f_\omega(t_0) \simeq 1 - i\omega t_0 + O\big(t_0^2\big). \tag{38}$$

On the other hand, Eq. (37) in the limit $\omega t_0 \ll 1$ provides

$$f_\omega(t_0) \simeq A_\omega (\omega t_0)^{\alpha+1/2} \frac{(1/2\sqrt{v_f/v_i})^\alpha}{\Gamma(\alpha+1)} + B_\omega (\omega t_0)^{-\alpha+1/2} \frac{(1/2\sqrt{v_f/v_i})^{-\alpha}}{\Gamma(-\alpha+1)}. \tag{39}$$

In this expression we can show that the scaling $(\omega t_0)^{\alpha+1/2}$ of the first term on the rhs eventually provides values of α which are incompatible with the self-consistent relation obeyed by $m_{\rm eff}(t)$ [Eq. (26)]. This imposes that $A_\omega = 0$. Comparing Eqs. (38) and (39) then implies that $B_\omega = B(\omega t_0)^{\alpha-1/2}(1 + B'\omega t_0/2)$, with B and B' prefactors independent of ω, such that

$$|f_\omega(t)|^2 \simeq |B|^2 \frac{t}{t_0}(\omega t_0)^{2\alpha}(1 + B'\omega t_0) J_{-\alpha}^2\left(\sqrt{\frac{v_f}{v_i}}\omega t\right). \tag{40}$$

The last step of the calculation consists in inserting this result into the self-consistent equation (26) obeyed by the effective mass $m_{\rm eff}(t)$. Matching both sides of this equation in the long-time limit imposes the value of a. The details of this procedure are presented in the Appendix for clarity. It leads to the only possible value $\alpha = \frac{1}{4}$, or equivalently $a = \frac{3}{16}$, so that

$$m_{\rm eff}(t) = \frac{3}{16}\frac{1}{t^2} \tag{41}$$

for quenches below the critical point. As shown in Fig. 4, this analytical result captures very well the numerical simulations at long time with, in particular, the correct prefactor $\frac{3}{16}$.

It should be noted that, according to the above analysis, both the scaling law $1/t^2$ and the prefactor $\frac{3}{16}$ follow from the property of scale invariance and are, in this sense, universal. In particular, the law (41) *a priori* holds for different types of frequency spectra. We have verified this by numerically computing $m_{\rm eff}(t)$ for a Gaussian spectrum $S_F(\omega) = (\sqrt{2\pi}/\gamma)\exp[-(\omega-\mu)/(2\gamma)^2]$. The result, shown in Fig. 4, converges as well to the prediction (41) (the timescale t_0 is even faster than for the Lorentzian spectrum in that case).

The value $\alpha = \frac{1}{4}$ also governs the asymptotic frequency-time scaling of the distribution function below the critical quench, which follows from Eq. (40):

$$|f_\omega(t)|^2 \sim \begin{cases} (t/t_0)^{1/2}, & \omega t \ll 1 \quad (42) \\ \left(\frac{1}{\omega t_0}\right)^{1/2} \cos^2(\omega t - \frac{\pi}{8}), & \omega t \gg 1. \quad (43) \end{cases}$$

To verify this analysis, in Fig. 5 we show the distribution $|f_\omega(t)|^2$ numerically obtained from Eq. (26). The plot shows $|f_0(t)|^2$, which indeed scales like $t^{1/2}$ at long time, in agreement with Eq. (42). The inset also shows $|f_\omega(t)|^2$ as a function of frequency for a fixed long time. It suggests $|f_\omega(t)|^2 \sim \omega^{-0.43}$, close to the prediction (43) [the small deviation from $\omega^{-1/2}$ observed here is due to finite-time effects, Eq. (43) strictly holding in the limits $\omega t_0 \ll 1$, $t/t_0 \gg 1$, and $\omega t \gg 1$]. In Fig. 6, finally, we plot the numerical distribution $\omega^{0.43}|f_\omega(t)|^2$ as a function of the product ωt for several values of ω. The curves at different frequencies all fall on a single one and oscillate as $\cos^2(\omega t - \pi/8)$, directly confirming the prediction (43).

As originally pointed out in [25,26,29] in the context of the $O(N)$ model, both asymptotic relations (42) and (43) can be seen as parts of the general scaling law $|f_\omega(t)|^2 = L^{1/2}(t)\mathcal{F}[\omega L(t)]$, which closely resembles the coarsening dynamics expected when quenching a classical system below a critical point. The quench process then gives rise, for $t > 0$, to the local formation of domains of size $L(t) \sim t$ growing linearly in time [55].

[2]The timescale t_0 is not universal and in particular depends on the form of the fluctuation spectrum. For the case of the Lorentzian spectrum with $\gamma = 0.1$ shown in Fig. 4, one has, e.g., $t_0 \simeq 300/\mu$. For a Gaussian spectrum, t_0 is much shorter.

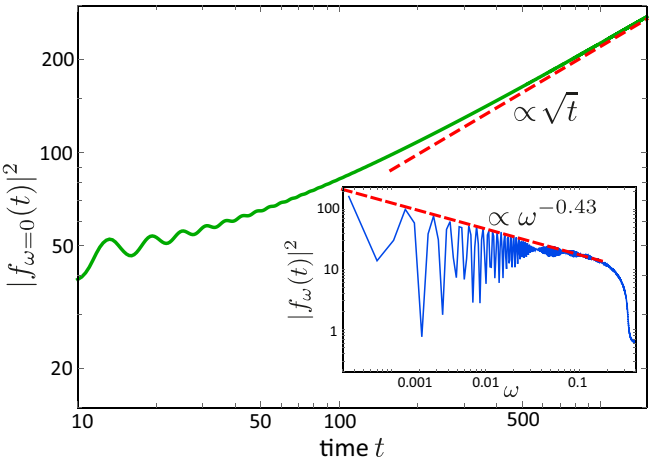

FIG. 5. Distribution function $|f_\omega(t)|^2$ at zero frequency as a function of time, obtained by solving numerically Eq. (26) for $m - m_c = -0.3$, $\lambda = 4$, and $\gamma = 0.1$. At long time $|f_0(t)|^2 \propto \sqrt{t}$, in agreement with Eq. (42). The inset shows the distribution function $|f_\omega(t)|^2$ as a function of ω. Here time is averaged over a small temporal window of width $\Delta t = 54$, centered around $t = 1420$. The numerics suggests $|f_\omega(t)|^2 \propto \omega^{-0.43}$ at small frequency, close to the prediction (43). The parameter units are the same as in Fig. 2.

VI. EXAMPLE: LIGHT IN ATOMIC VAPORS

A representative example of nonlinear dispersive medium for light is vapors of hot atoms optically illuminated in the vicinity of an atomic resonance. Recently, this platform was extensively used to investigate a variety of nonequilibrium phenomena with light [20,40–45,56–58]. In this section we discuss under what conditions they could be exploited to also explore the dynamical phase transition studied in the present paper. Note that here we do not aim to provide an exhaustive description of this system, but merely to give an example

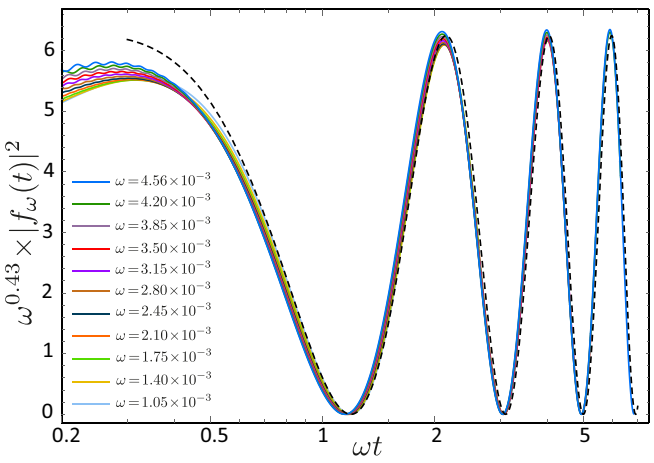

FIG. 6. Rescaled distribution $\omega^{0.43}|f_\omega(t)|^2$ as a function of the product ωt for several values of ω, obtained by solving numerically Eq. (26) for $m - m_c = -0.3$, $\lambda = 4$, and $\gamma = 0.1$. The dashed curve is the theoretical prediction (43), in which the only free parameter is the (nonuniversal) prefactor. The parameter units are the same as in Fig. 2.

of practical quench protocol and to emphasize its possible limitations.

Let consider an ensemble of two-level atoms consisting of a ground state $|g\rangle$ and an excited state $|e\rangle$. We denote by ω_0 the resonance frequency between these two states and by Γ the decay rate of the excited state. According to the discussion in Sec. III B, observing the DPT requires us to perform a temporal change of the group velocity v in the vapor from v_i to v_f, the critical quench being achieved for the ratio $v_f/v_i = v_f/v_i|_c$ defined by Eq. (28). When $v_f/v_i < v_f/v_i|_c$, the postquench optical beam lies in the normal dynamical phase, characterized by a finite effective mass and a finite correlation length, as discussed in Sec. IV. When $v_f/v_i > v_f/v_i|_c$, the beam instead lies in the coarsening phase and the effective mass decays algebraically (see Sec. V).

In order to be able to observe the DPT in practice, three constraints must be satisfied: (i) Because $v_f/v_i|_c > 1$ [see Eq. (28)], crossing the DPT requires the postquench velocity v_f to be larger than the prequench velocity v_i, (ii) the prequench and postquench dispersion parameters should obey the phase-matching condition (25), and (iii) the nonlinear parameter λ should be positive. In an atomic vapor, a temporal quench of the dispersion parameters can be achieved by exploiting the dependence of the group velocity v and the quadratic dispersion D upon the detuning $\Delta \equiv \omega - \omega_0$ of the laser exciting the transition: A change from Δ_i to Δ_f changes $v_i \equiv v(\Delta_i)$ to $v_f \equiv v(\Delta_f)$ and similarly $D_i \equiv D(\Delta_i)$ to $D_f \equiv D(\Delta_f)$. To express these quantities, we assume that the vapor is dilute so that its refractive index n depends on the detuning as $n(\Delta) \equiv 1 - (6\pi\rho\Gamma/2k_0^3)\Delta/(\Delta^2 + \Gamma^2/4)$, where ρ is the atom density and $k_0 \equiv \omega_0/c$ [59]. The group velocity and the quadratic dispersion parameter follow from $v \equiv (\partial k/\partial\omega)^{-1}$ and $D \equiv \frac{1}{2}(\partial^2 k^2/\partial\omega^2)$, respectively, where $k \equiv n\omega/c$ is the wave number in the vapor.

A possible configuration satisfying the above conditions (i)–(iii) is illustrated in Fig. 7(a), where we show the group velocity v and the product Dv as a function of Δ: By quenching the detuning from the initial value $\Delta_i \simeq (-\sqrt{3} + \Gamma/2\omega_0)\Gamma/2$ to a final one $\Delta_f < 0$ such that $|\Delta_f| \gg \Gamma/2$, one simultaneously realizes $v_f/v_i > 1$, $D_f v_f = D_i v_i$, and $\lambda > 0$ [the latter condition follows from the proportionality relation $\lambda \propto g \propto -\Delta_f$ in an atomic vapor; see Eq. (44) below]. Within this protocol, it is also required that the laser power is increased from a small to a finite s_0 value [see Eq. (44) below] to realize the interaction quench.

In the configuration described above, the two dynamical phases of the DPT can be probed by varying the ratio v_f/v_i via Δ_f around the critical value $v_f/v_i|_c$. The latter is identified by the relation (28), which is a function of the nonlinear parameter $\lambda \equiv 4gID_f v_f^2/k_0^2$. In an ensemble of two-level atoms, the product gI is conveniently expressed in terms of the resonant saturation parameter s_0, which is the ratio of the laser intensity to the intensity required to saturate the atomic transition [60]:

$$gI = -\frac{6\pi\rho}{k_0}\frac{\Delta_f\Gamma^3/4}{(\Delta_f^2 + \Gamma^2/4)^2}s_0. \tag{44}$$

Inserting this relation into Eq. (28) and making explicit the Δ_f dependence of the ratio v_f/v_i, we infer the phase

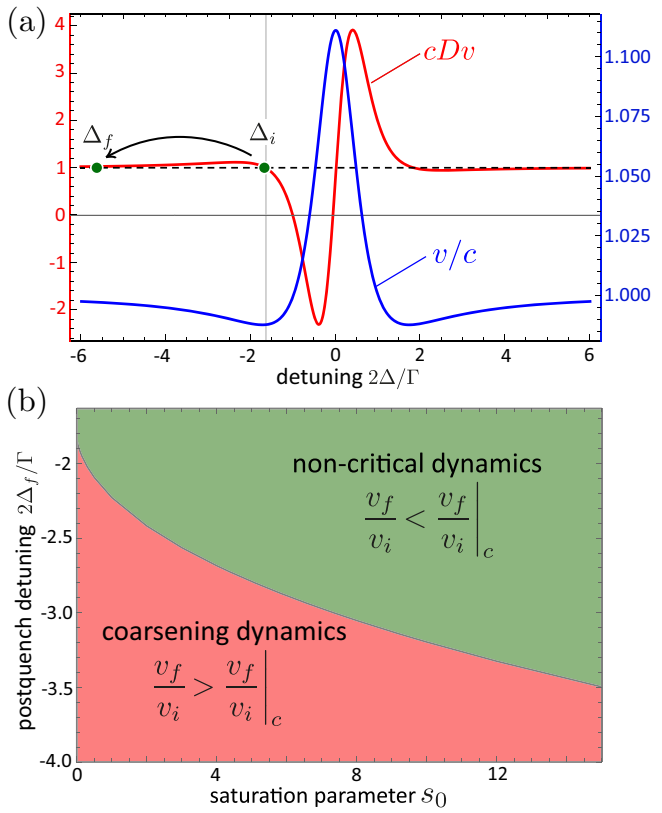

FIG. 7. (a) Detuning dependence of the group velocity v and of the product Dv (with D the quadratic dispersion) in a dilute atomic vapor. By choosing $\Delta_i \simeq (-\sqrt{3}+\Gamma/2\omega_0)\Gamma/2$ and quenching to a large negative detuning Δ_f, one simultaneously satisfies the conditions $v_f/v_i > 1$, $D_f v_f = D_i v_i$, and $\Delta_f < 0$ required to observe the DPT. The horizontal dashed line is a guide to the eye, identifying the condition $D_f v_f = D_i v_i$. (b) Phase diagram of the DPT in the (s_0, Δ_f) plane for the choice $\Delta_i \simeq (-\sqrt{3}+\Gamma/2\omega_0)\Gamma/2$. In both plots, we take $6\pi\rho/k_0^3 = 10^{-2}$ for the atomic density and $2\omega_0/\Gamma = 10$ for the quality factor of the transition.

diagram of the DPT in the plane (s_0, Δ_f) for the atomic vapor [see Fig. 7(b)]. For a given laser intensity s_0, this diagram suggests that the DPT can be crossed by choosing a large enough (negative) value of the postquench detuning. As the nonlinearity is increased (larger s_0), larger detunings are required because of the increase of the critical ratio $v_f/v_i|_c$. Note that in this simple model, we have neglected a number of effects such as Doppler broadening or absorption. While the impact of Doppler broadening should be limited by operating at large detuning, residual absorption is always present and it is not clear how it will affect the physics of the DPT.

VII. CONCLUSION

In this work we have provided theoretical evidence for a dynamical phase transition for fluctuating optical beams propagating in nonlinear dispersive media. The existence of this DPT fundamentally relies on a mapping between the nonlinear dispersive wave equation in the slowly varying envelope approximation and a massive φ^4 theory. From this observation, the DPT can be triggered by a temporal change of the dispersion parameters, which simulates a quench in the corresponding φ^4 model. From this perspective, we have identified the precise phase-matching condition required for the DPT to occur. Generally speaking, the idea of applying temporal quenches to dielectric media has recently gained more and more interest in optics [52], even though so far it has not been explored much in nonlinear media.

By numerically and theoretically investigating the optical DPT in the vicinity of the critical point, we have connected its critical exponent to the one of equilibrium quantum phase transitions in the φ^4 theory. Slightly above the critical point, we have also disclosed a dimensional crossover of the critical exponent. This crossover is a characteristic feature of the optical problem, stemming from the peculiar shape of the fluctuation spectrum, which competes with the infrared physics of the transition by favoring a finite optical frequency. Below the transition, we have numerically and theoretically described the postquench coarsening dynamics. In particular, because it describes a DPT with quantumlike critical properties, our analytical approach in this regime differs from those of previous work [29], which focused on a classical deep-quench limit.

The DPT discussed in this work is an example of a fixed point arising in the short-time prethermal regime of a weakly nonlinear system [30] and thus does not involve any inelastic scattering processes. Such processes are nevertheless present in the original nonlinear dispersive equation, and their onset corresponds to a breakdown of the factorization ansatz (16). They are expected to make the system deviate from the fixed point at long time and eventually to thermalize it. The timescale where this thermalization occurs is expected to scale as $1/g^2$ and can therefore be very long for a weak nonlinearity. Nevertheless, while the crossover from prethermalization to thermalization in quantum fluids has been recently studied in a few cases [61–64], its general description in situations where a prethermal DPT is present remains an open problem.

ACKNOWLEDGMENTS

Financial support from the Agence Nationale de la Recherche (Grant No. ANR-19-CE30-0028-01 CONFOCAL) is gratefully acknowledged. The author is indebted to Quentin Glorieux, Dominique Delande, Maxime Jacquet, and Giovanni Martone for helpful discussions.

APPENDIX: DETERMINATION OF THE SCALING FACTOR *A*

To find the value of the scaling factor a, we use that, below the critical point, the solutions $m_{\rm eff}(t) = a/t^2$ for the effective mass and Eq. (40) for the distribution function are related through Eq. (26) at long enough time. Introducing the rescaled time $x \equiv \sqrt{v_f/v_i}\,t$, Eq. (26) reads

$$\frac{v_f}{v_i}\frac{a}{x^2} = m + \Lambda R(x), \tag{A1}$$

where $\Lambda \equiv \lambda|B|^2\sqrt{v_i/v_f}t_0^{2\alpha-1}/2$ (with $\alpha = \sqrt{1/4-a}$) and

$$R(x) = x\int_{-\infty}^{\infty}\frac{d\omega}{2\pi}\frac{2\gamma}{(\omega-1)^2+\gamma^2}\omega^{2\alpha}(1+B't_0\omega)J_{-\alpha}^2(\omega x). \tag{A2}$$

Then we follow the method proposed in [29] and expand $R(x)$ at large x. The expansion reads

$$R(x) = C_0(\alpha,B') + \frac{C_1(\alpha)}{x^{2\alpha}} + \frac{C_2(\alpha,B')}{x^{2\alpha+1}} + \frac{C_3(\alpha,B')}{x^2} + \cdots. \tag{A3}$$

The coefficients C_i of this expansion all depend on α and B', except C_1 (they also all depend on γ, but this dependence is not relevant in the reasoning).

In order for Eq. (A1) to be satisfied, both prefactors C_1 and C_2 should be zero. Since C_1 is independent of B', the condition $C_1(\alpha) = 0$ is the one that restricts the possible values of α. From the expansion of $R(x)$ at large x we find

$$C_1(\alpha) \propto \frac{1}{\Gamma(1/2-2\alpha)\Gamma(1/2-\alpha)}, \tag{A4}$$

where Γ is the gamma function. This leads to the possible sets of values $\alpha = \{1/4+n/2\}$ or $\alpha = \{1/2+n\}$, with n an integer. Among these values, only the one $\alpha = 1/2$ is compatible with a positive effective mass, i.e., $a > 0$. The condition $C_2(\alpha, B') = 0$, on the other hand, enforces the value of B', while the equations $m + \Lambda C_0(\alpha, B') = 0$ and $\Lambda C_3(\alpha, B') = (v_f/v_i)a$ fix the values of B and t_0.

[1] P. Jurcevic, H. Shen, P. Hauke, C. Maier, T. Brydges, C. Hempel, B. P. Lanyon, M. R. Heyl, R. Blatt, and C. F. Roos, Direct observation of dynamical quantum phase transitions in an interacting many-body system, Phys. Rev. Lett. **119**, 080501 (2017).

[2] N. Fläschner, D. Vogel, M. Tarnowski, B. S. Rem, D.-S. Lühmann, M. Heyl, J. C. Budich, L. Mathey, K. Sengstock, and C. Weitenberg, Observation of dynamical vortices after quenches in a system with topology, Nat. Phys. **14**, 265 (2018).

[3] M. Heyl, Dynamical quantum phase transitions: A review, Rep. Prog. Phys. **81**, 054001 (2018).

[4] J. Berges, A. Rothkopf, and J. Schmidt, Nonthermal fixed points: Effective weak coupling for strongly correlated systems far from equilibrium, Phys. Rev. Lett. **101**, 041603 (2008).

[5] B. Nowak, D. Sexty, and T. Gasenzer, Superfluid turbulence: Nonthermal fixed point in an ultracold Bose gas, Phys. Rev. B **84**, 020506(R) (2011).

[6] M. Prüfer, P. Kunkel, H. Strobel, S. Lannig, D. Linnemann, C.-M. Schmied, J. Berges, T. Gasenzer, and M. K. Oberthaler, Observation of universal dynamics in a spinor Bose gas far from equilibrium, Nature (London) **563**, 217 (2018).

[7] S. Erne, R. Bücker, T. Gasenzer, J. Berges, and J. Schmiedmayer, Universal dynamics in an isolated one-dimensional Bose gas far from equilibrium, Nature (London) **563**, 225 (2018).

[8] C. Eigen, J. A. P. Glidden, R. Lopes, E. A. Cornell, R. P. Smith, and Z. Hadzibabic, Universal prethermal dynamics of Bose gases quenched to unitarity, Nature (London) **563**, 221 (2018).

[9] C.-M. Schmied, A. N. Mikheev, and T. Gasenzer, Nonthermal fixed points: Universal dynamics far from equilibrium, Int. J. Mod. Phys. A **34**, 1941006 (2019).

[10] J. Marino, M. Eckstein, M. S. Foster, and A. M. Rey, Dynamical phase transitions in the collisionless pre-thermal states of isolated quantum systems: Theory and experiments, Rep. Prog. Phys. **85**, 116001 (2022).

[11] J. Berges, S. Borsányi, and C. Wetterich, Prethermalization, Phys. Rev. Lett. **93**, 142002 (2004).

[12] T. Mori, T. N. Ikeda, E. Kaminishi, and M. Ueda, Thermalization and prethermalization in isolated quantum systems: A theoretical overview, J. Phys. B **51**, 112001 (2018).

[13] P.-É. Larré, D. Delande, and N. Cherroret, Postquench prethermalization in a disordered quantum fluid of light, Phys. Rev. A **97**, 043805 (2018).

[14] G. I. Martone, P.-E. Larré, A. Fabbri, and N. Pavloff, Momentum distribution and coherence of a weakly interacting Bose gas after a quench, Phys. Rev. A **98**, 063617 (2018).

[15] K. Mallayya, M. Rigol, and W. De Roeck, Prethermalization and thermalization in isolated quantum systems, Phys. Rev. X **9**, 021027 (2019).

[16] T. Bardon-brun, S. Pigeon, and N. Cherroret, Classical Casimir force from a quasi-condensate of light, Phys. Rev. Res. **2**, 013297 (2020).

[17] M. Gring, M. Kuhnert, T. Langen, T. Kitagawa, B. Rauer, M. Schreitl, I. Mazets, D. A. Smith, E. Demler, and J. Schmiedmayer, Relaxation and prethermalization in an isolated quantum system, Science **337**, 1318 (2012).

[18] T. Langen, R. Geiger, M. Kuhnert, B. Rauer, and J. Schmiedmayer, Local emergence of thermal correlations in an isolated quantum many-body system, Nat. Phys. **9**, 640 (2013).

[19] Y. Tang, W. Kao, K.-Y. Li, S. Seo, K. Mallayya, M. Rigol, S. Gopalakrishnan, and B. L. Lev, Thermalization near integrability in a dipolar quantum Newton's cradle, Phys. Rev. X **8**, 021030 (2018).

[20] M. Abuzarli, N. Cherroret, T. Bienaimé, and Q. Glorieux, Nonequilibrium pre-thermal states in a two-dimensional photon fluid, Phys. Rev. Lett. **129**, 100602 (2022).

[21] A. Das, K. Sengupta, D. Sen, and B. K. Chakrabarti, Infinite-range Ising ferromagnet in a time-dependent transverse magnetic field: Quench and ac dynamics near the quantum critical point, Phys. Rev. B **74**, 144423 (2006).

[22] B. Sciolla and G. Biroli, Dynamical transitions and quantum quenches in mean-field models, J. Stat. Mech. **2011**, P11003.

[23] N. Defenu, T. Enss, M. Kastner, and G. Morigi, Dynamical critical scaling of long-range interacting quantum magnets, Phys. Rev. Lett. **121**, 240403 (2018).

[24] A. Lerose A, B. Žunkovič, J. Marino, A. Gambassi, and A. Silva, Impact of nonequilibrium fluctuations on prethermal dynamical phase transitions in long-range interacting spin chains, Phys. Rev. B **99**, 045128 (2019).

[25] A. Chandran, A. Nanduri, S. S. Gubser, and S. L. Sondhi, Equilibration and coarsening in the quantum $O(N)$ model at infinite N, Phys. Rev. B **88**, 024306 (2013).

[26] B. Sciolla and G. Biroli, Quantum quenches, dynamical transitions, and off-equilibrium quantum criticality, Phys. Rev. B **88**, 201110(R) (2013).

[27] P. Smacchia, M. Knap, E. Demler, and A. Silva, Exploring dynamical phase transitions and prethermalization with quantum noise of excitations, Phys. Rev. B **91**, 205136 (2015).

[28] A. Chiocchetta, A. Gambassi, S. Diehl, and J. Marino, Dynamical crossovers in prethermal critical states, Phys. Rev. Lett. **118**, 135701 (2017).

[29] A. Maraga, A. Chiocchetta, A. Mitra, and A. Gambassi, Aging and coarsening in isolated quantum systems after a quench: Exact results from the quantum $O(N)$ model with $N \to \infty$, Phys. Rev. E **92**, 042151 (2015).

[30] A. Chiocchetta, M. Tavora, A. Gambassi, and A. Mitra, Short-time universal scaling in an isolated quantum system after a quench, Phys. Rev. B **91**, 220302(R) (2015).

[31] A. Chiocchetta, M. Tavora, A. Gambassi, and A. Mitra, Short-time universal scaling and light-cone dynamics after a quench in an isolated quantum system in d spatial dimension, Phys. Rev. B **94**, 134311 (2016).

[32] J. C. Halimeh and M. F. Maghrebi, Quantum aging and dynamical universality in the long-range $O(N \to \infty)$ model, Phys. Rev. E **103**, 052142 (2021).

[33] J. Zhang, G. Pagano, P. W. Hess, A. Kyprianidis, P. Becker, H. Kaplan, A. V. Gorshkov, Z.-X. Gong, and C. Monroe, Observation of a many-body dynamical phase transition with a 53-qubit quantum simulator, Nature (London) **551**, 601 (2017).

[34] J. A. Muniz, D. Barberena, R. J. Lewis-Swan, D. J. Young, J. R. K. Cline, A. M. Rey, and J. K. Thompson, Exploring dynamical phase transitions with cold atoms in an optical cavity, Nature (London) **580**, 602 (2020).

[35] S. Smale, P. He, B. A. Olsen, K. G. Jackson, H. Sharum, S. Trotzky, J. Marino, A. M. Rey, and J. H. Thywissen, Observation of a transition between dynamical phases in a quantum degenerate Fermi gas, Sci. Adv. **5** eaax1568 (2019).

[36] H.-X. Yang, T. Tian, Y.-B. Yang, L.-Y. Qiu, H.-Y. Liang, A.-J. Chu, C. B. Dağ, Y. Xu, Y. Liu, and L.-M. Duan, Observation of dynamical quantum phase transitions in a spinor condensate, Phys. Rev. A **100**, 013622 (2019).

[37] T. Tian, H.-X. Yang, L.-Y. Qiu, H.-Y. Liang, Y.-B. Yang, Y. Xu, and L.-M. Duan, Observation of dynamical quantum phase transitions with correspondence in an excited state phase diagram, Phys. Rev. Lett. **124**, 043001 (2020).

[38] I. Carusotto and C. Ciuti, Quantum fluids of light, Rev. Mod. Phys. **85**, 299 (2013).

[39] Q. Glorieux, T. Aladjidi, P. D. Lett, and R. Kaiser, Hot atomic vapors for nonlinear and quantum optics, New J. Phys. **25**, 051201 (2023).

[40] C. Sun, S. Jia, C. Barsi, S. Rica, A. Picozzi, and J. W. Fleischer, Observation of the kinetic condensation of classical waves, Nat. Phys. **8**, 470 (2012).

[41] N. Šantić, A. Fusaro, S. Salem, J. Garnier, A. Picozzi, and R. Kaiser, Nonequilibrium precondensation of classical waves in two dimensions propagating through atomic vapors, Phys. Rev. Lett. **120**, 055301 (2018).

[42] J. Steinhauer, M. Abuzarli, T. Aladjidi, T. Bienaimé, C. Piekarski, W. Liu, E. Giacobino, A. Bramati, and Q. Glorieux, Analogue cosmological particle creation in an ultracold quantum fluid of light, Nat. Commun. **13**, 2890 (2022).

[43] P. Azam, A. Griffin, S. Nazarenko, and R. Kaiser, Vortex creation, annihilation, and nonlinear dynamics in atomic vapors, Phys. Rev. A **105**, 043510 (2022).

[44] G. Martone and N. Cherroret, Time translation symmetry breaking in an isolated spin-orbit-coupled fluid of light, Phys. Rev. Lett. **131**, 013803 (2023).

[45] M. Abobaker, W. Liu, T. Aladjidi, A. Bramati, and Q. Glorieux, Turbulent dynamics in two-dimensional paraxial fluid of light, arXiv:2211.08441.

[46] G. Van Simaeys, P. Emplit, and M. Haelterman, Experimental demonstration of the Fermi-Pasta-Ulam recurrence in a modulationally unstable optical wave, Phys. Rev. Lett. **87**, 033902 (2001).

[47] A. Mussot, A. Kudlinski, M. Droques, P. Szriftgiser, and N. Akhmediev, Fermi-Pasta-Ulam recurrence in nonlinear fiber optics: The role of reversible and irreversible losses, Phys. Rev. X **4**, 011054 (2014).

[48] A. Mussot, C. Naveau, M. Conforti, A. Kudlinski, F. Copie, P. Szriftgiser, and S. Trillo, Fibre multi-wave mixing combs reveal the broken symmetry of Fermi-Pasta-Ulam recurrence, Nat. Photonics **12**, 303 (2018).

[49] N. N. Rosanov, *Spatial Hysteresis and Optical Patterns* (Springer, New York, 2002).

[50] H. Kleinert and V. Schulte-Frohlinde, *Critical Properties of ϕ^4 Theories* (World Scientific, Singapore, 2001).

[51] M. Moshe and J. Zinn-Justin, Quantum field theory in the large N limit: A review, Phys. Rep. **385**, 69 (2003).

[52] E. Galiffi, R. Tirole, S. Yin, H. Li, S. Vezzoli, P. A. Huidobro, M. G. Silveirinha, R. Sapienza, A. Alù, and J. B. Pendry, Photonics of time-varying media, Adv. Photon. **4**, 014002 (2022).

[53] K. B. Blagoev, F. Cooper, J. F. Dawson, and B. Mihaila, Schwinger-Dyson approach to nonequilibrium classical field theory, Phys. Rev. D **64**, 125003 (2001).

[54] S. Sotiriadis and J. Cardy, Quantum quench in interacting field theory: A self-consistent approximation, Phys. Rev. B **81**, 134305 (2010).

[55] G. Biroli, in *Strongly Interacting Quantum Systems Out of Equilibrium*, edited by T. Giamarchi, A. J. Millis, O. Parcollet, H. Saleur, and L. F. Cugliandolo, Proceedings of the Les Houches Summer School of Theoretical Physics, XCIX, 2012 (Oxford University Press, Oxford, 2016).

[56] D. Vocke, T. Roger, F. Marino, E. M. Wright, I. Carusotto, M. Clerici, and D. Faccio, Experimental characterization of nonlocal photon fluids, Optica **2**, 484 (2015).

[57] Q. Fontaine, T. Bienaimé, S. Pigeon, E. Giacobino, A. Bramati, and Q. Glorieux, Observation of the Bogoliubov dispersion in a fluid of light, Phys. Rev. Lett. **121**, 183604 (2018).

[58] G. I. Martone, T. Bienaimé, and N. Cherroret, Spin-orbit-coupled fluids of light in bulk nonlinear media, Phys. Rev. A **104**, 013510 (2021).

[59] O. Morice, Y. Castin, and J. Dalibard, Refractive index of a dilute Bose gas, Phys. Rev. A **51**, 3896 (1995).

[60] H. da Silva, R. Kaiser, and T. Macrì, Static and dynamic properties of self-bound droplets of light in hot vapors, Phys. Rev. A **107**, 033519 (2023).

[61] M. Buchhold and S. Diehl, Kinetic theory for interacting Luttinger liquids, Eur. Phys. J. D **69**, 224 (2015).

[62] M. Buchhold, M. Heyl, and S. Diehl, Prethermalization and thermalization of a quenched interacting Luttinger liquid, Phys. Rev. A **94**, 013601 (2016).

[63] M. Van Regemortel, H. Kurkjian, M. Wouters, and I. Carusotto, Prethermalization to thermalization crossover in a dilute Bose gas following an interaction ramp, Phys. Rev. A **98**, 053612 (2018).

[64] C. Duval and N. Cherroret, Quantum kinetics of quenched two-dimensional Bose superfluids, Phys. Rev. A **107**, 043305 (2023).